Original Russian Text © P.E. Shtykovskiy, M.R. Gilfanov, 2007, published in Pis'ma v Astronomicheskii Zhurnal, 2007, Vol. 33, No. 5, pp. 340–351.

# High-Mass X-ray Binaries and the Spiral Structure of the Host Galaxy

**P. E. Shtykovskiy[1,2*] and M. R. Gilfanov[2,3]**

[1] *Space Research Institute, Russian Academy of Sciences, Profsoyuznaya ul. 84/32, Moscow 117997, Russia*
[2] *Max-Planck-Institut für Astrophysik, Karl-Schwarzschild-Str. 1, Postfach 1317, D-85741 Garching, Germany*
[3] *Space Research Institute, Russian Academy of Sciences, Profsoyuznaya ul. 84/32, Moscow 117810, Russia*

Received December 12, 2006

**Abstract**—We investigate the manifestation of the spiral structure in the distribution of high-mass X-ray binaries (HMXBs) over the host galaxy. We construct the simplest kinematic model. It shows that the HMXBs should be displaced relative to the spiral structure observed in such traditional star formation rate indicators as the H$\alpha$ and far-infrared emissions because of their finite lifetimes. Using Chandra observations of M51, we have studied the distribution of X-ray sources relative to the spiral arms of this galaxy observed in H$\alpha$. Based on K-band data and background source number counts, we have separated the contributions from high-mass and low-mass X-ray binaries and active galactic nuclei. In agreement with model predictions, the distribution of HMXBs is wider than that of bright H II regions concentrated in the region of ongoing star formation. However, the statistical significance of this result is low, as is the significance of the concentration of the total population of X-ray sources to the spiral arms. We also predict the distribution of HMXBs in our Galaxy in Galactic longitude. The distribution depends on the mean HMXB age and can differ significantly from the distributions of such young objects as ultracompact H II regions.

PACS numbers : 97.30.Eh
**DOI:** 10.1134/S1063773707050039

Key words: *stars—variable and peculiar, high-mass X-ray binaries, spiral structure, M51, Galaxy.*

## INTRODUCTION

Chandra and XMM-Newton X-ray observations of nearby galaxies have revealed rich populations of compact X-ray sources in them (see, e.g., Fabbiano 2006; Kilgard et al. 2005). Their spectral analysis, flux variability, luminosity functions, and spatial distribution make it possible to identify them with known (in our Galaxy) classes of objects—high-mass and low-mass X-ray binaries, supernova remnants, ultrasoft X-ray sources, and to distinguish a hitherto unknown class of ultrabright X-ray sources.

From the standpoint of their relation to star formation, the X-ray sources can be divided into two groups: young objects, such as high-mass X-ray binaries (HMXBs) and supernova remnants (SNRs), and old objects, such as low-mass X-ray binaries (LMXBs). It would be natural to expect the former to concentrate in regions of recent star formation and the latter to follow the galactic stellar mass distribution. Indeed, Chandra observations of nearby galaxies show that the populations of X-ray sources in star-forming galaxies differ radically from those in elliptical galaxies. This is particularly clearly seen when the luminosity functions of these sources are analyzed: the luminosity functions for the former are in the form of a power law with an index of 1.6, as for the HMXBs in our Galaxy, while those for the latter are similar in form to the luminosity function of LMXBs in our Galaxy (Grimm et al. 2003; Gilfanov 2004).

In nearby spiral galaxies, two components should be observed in the distribution of X-ray sources: HMXBs concentrating to the spiral arms and LMXBs distributed more smoothly with the maximum density at the galactic center. On the one hand, Chandra observations of such galaxies as M51 and M101 suggest that the X-ray sources actually concentrate to the spiral arms. However, a more detailed analysis indicates that, in reality, the picture is more complex. First, HMXBs reflect the star formation in a galaxy that took place $\sim$5–60 Myr ago, i.e., strictly speaking, they are not a star formation rate (SFR) indicator (Shtykovskiy and Gilfanov 2005). Such times may turn out to be important from the standpoint of galactic dynamics, since the characteristic revolution time of the stars in a typical spiral galaxy is $\sim$200 Myr. As a result, the spiral structure observed in the

*E-mail: pav_sht@hea.iki.rssi.ru

HMXB distribution will be distorted and displaced relative to that observed, for example, in H$\alpha$. On the other hand, the density contrast between the arms and the interarm space in the stellar population of certain galaxies can reach $\sim$3. This will give rise to a spiral structure in the old population of LMXBs as well.

In this paper, we construct a kinematic model for the spatial distribution of X-ray binaries in a spiral galaxy, compare its predictions with Chandra observations of M51, and make predictions for our Galaxy.

## THE SPIRAL STRUCTURE IN VARIOUS SFR INDICATORS

The basic principles of the modern theory of spiral structure in galaxies were laid down by Lin and Shu (1964, 1966) and Lin et al. (1969), who suggested the hypothesis of a quasi-stationary density wave. According to this hypothesis, the spiral structure of a galaxy is a manifestation of the density wave—a stellar disk and gas density perturbation that propagates through the galaxy and that does not decay for a long period. Although the reasons why a stationary density wave emerges and is maintained are unknown, there are many candidates for their role, such as the influence of a neighboring galaxy, asymmetry at the galactic center, etc. Since the velocity dispersion in the interstellar gas is comparatively low, the amplitude of the density wave triggered by a gravitational potential perturbation can be large. In contrast, the amplitude of the density wave in the stellar disk should be small (at least for an isolated galaxy). Moreover, a shock wave leading to a very narrow zone of gas compression with a large density jump can generally emerge in the gas (Roberts 1969). The gas compression triggers star formation in it; as a result, young stars producing a distinct galactic spiral structure in the visible range are formed.

In addition to the visible range, the spiral structure can also be observed in many other SFR, stellar mass, and gas indicators. The H$\alpha$, ultraviolet, and far-infrared emissions produced by massive stars, the near-infrared emission from old stars, the 21-cm HI emission, and the CO emission are the most important ones. Simple considerations suggest that the spiral structure will be different in different indicators. For example, the H$\alpha$ emission originates in H II regions containing young stars with masses $\gtrsim 10M_\odot$, while the ultraviolet emission is associated with the photospheric emission of stars from a wide mass range (Kennicutt 1998). Since the angular velocities of the stellar disk and the density wave are different, young stars are displaced from the density wave shock front with time. Due to short lifetimes of the massive stars responsible for the H$\alpha$ emission, $\lesssim 20$ Myr, its peak should lie not far from the spiral density wave front. On the other hand, the less massive stars responsible for the ultraviolet emission have lifetimes up to 100 Myr and can be displaced significantly from their birthplaces. As a result, the spiral structure in the ultraviolet will be considerably wider than that in H$\alpha$. Displacements of this kind between various indicators were actually observed, for example, between H$\alpha$ and the ultraviolet in M51 (Petit et al. 1996), HI and the nonthermal radio continuum in M51 and M83 (Tilanus and Allen 1991), etc.

The situation with HMXBs is similar to that described above. Indeed, the lifetime of an optical counterpart with a mass of $\sim 8M_\odot$ is $\sim$40 Myr, i.e., HMXBs reflect the star formation that took place several tens of Myr ago. A clear example of this, though unrelated to the spiral structure, is the absence of any correlation between the surface density of HMXBs and the H$\alpha$ emission intensity in the Large Magellanic Cloud (Shtykovskiy and Gilfanov 2005).

### *The Spiral Structure in the Distribution of High-Mass X-ray Binaries*

To summarize the aforesaid, we conclude that the following factors affect the spatial distribution of HMXBs.

(i) The spatial distribution of star-forming regions. The theory of density waves and observations of spiral galaxies show that a logarithmic spiral can serve as a good approximation for the location of the spiral density wave front. The location of a spiral arm is then specified in polar coordinates $(r, \Theta)$ by the relation

$$\Theta - \Theta_0 = \ln(r/r_0)/\tan\psi, \qquad (1)$$

where $\psi$ is the angle between the spiral and the tangent to the circumference called the pitch angle and $(r_0, \Theta_0)$ is a point on the spiral, for example, its origin. We assume that the star formation takes place in a narrow region along this spiral.

(ii) The dynamics of HMXBs. The HMXBs born at the shock front are drawn into the overall motion of the stellar disk in accordance with the galactic rotation curve. To a first approximation, it can be represented as the motion in circular orbits around the galactic center. The spiral density wave rotates with the pattern speed $\Omega_\mathrm{p}$ in the same direction as the stellar disk. The HMXB locations relative to the instantaneous location of the spiral density wave front, which is initially equal to zero, in time $\tau$ is then given by the following equation:

$$\Delta\Theta = (\Omega(r) - \Omega_\mathrm{p})\tau, \qquad (2)$$

where $\Delta\Theta$ is the displacement of the objects relative to the instantaneous location of the density

wave and $\Omega(r)$ is the galactic rotation curve. In other words, this formula gives the locations of objects with age $\tau$ relative to the currently observed star-forming region. Obviously, the HMXBs move faster than the density wave within the corotation radius $r_{\rm cr}$ ($\Omega(r_{\rm cr}) = \Omega_{\rm p}$) and lag behind it outside $r_{\rm cr}$.

In this formula, the gravitational field perturbation in the galaxy and the fact that the stars move in epicyclic orbits, not in circular ones, are ignored. To accurately describe the dynamics of the various components of a spiral galaxy, we must also consider the dynamics of gas clouds and the star formation in them under the effect of gravitational instability. Models of this interaction (see, e.g., Leisawitz and Bash 1982; Roberts and Stewart 1987) yield contradictory results: young stars will move almost along the spiral arm for a certain time in some of the models and will be rapidly displaced from it in other models.

(iii) The evolution of the HMXB number with time elapsed since the star formation event. A detailed investigation of this question is a difficult task that requires developing population synthesis models and is beyond the scope of this paper. Here, we only briefly note the main factors that specify the evolution time scale of the population of HMXBs. First, this is the time it takes for a black hole or a neutron star to be formed. Here, two natural time scales can be identified: the lifetime of the most massive star ($\approx 100 M_\odot$) corresponding to the formation of the first compact object (black hole), $t_{\rm min} \approx 2$–$3$ Myr, and the lifetime of the least massive star ($\approx 8 M_\odot$) capable of forming a compact object—the formation time of the last neutron star, $t_{\rm max} \approx 40$ Myr. The evolution of the companion star until the onset of an active phase, mass accretion onto the compact object, is of no less importance. The duration of this phase can also be rather long, up to several tens of Myr, depending on the mass of the companion star. In addition, the duration of the X-ray activity phase, which should be much shorter than the first two phases, $10^3$–$10^6$ Myr, must be taken into account. As a result, the maximum age for a HMXB can reach more than 40 Myr. This is also confirmed by observations: for example, analysis of the population of HMXBs in the Magellanic Clouds showed that binaries with ages up to $\sim$60 Myr could be present among them (Shtykovskiy and Gilfanov 2007). Below, as the time scale for the existence of a HMXB population, we use both a conservative estimate of $e_{\rm max} \approx 40$ Myr and larger values, demonstrating the magnitude of the effect in the latter case for the oldest binaries.

It is also worth noting that the displacement of HMXBs relative to other SFR indicators observed in galaxies at distances $\gtrsim 1$ Mpc can be slightly smaller than that in nearby galaxies. Indeed, when X-ray binaries are observed in distant galaxies, there is a selection effect: the brightest objects are selected. Since the luminosity of a HMXB is related to the mass of its optical counterpart (Postnov 2003), a mass selection effect also arises, i.e., predominantly the highest-mass and, accordingly, youngest stars for which the displacement from the spiral arms is smaller, will be observed. However, apart from the mass of the counterpart, the luminosity also depends on the orbital size. This reduces the selection effect and increases the contribution from "old" HMXBs to the observed population of X-ray sources. A detailed analysis of this effect is beyond the scope of this paper.

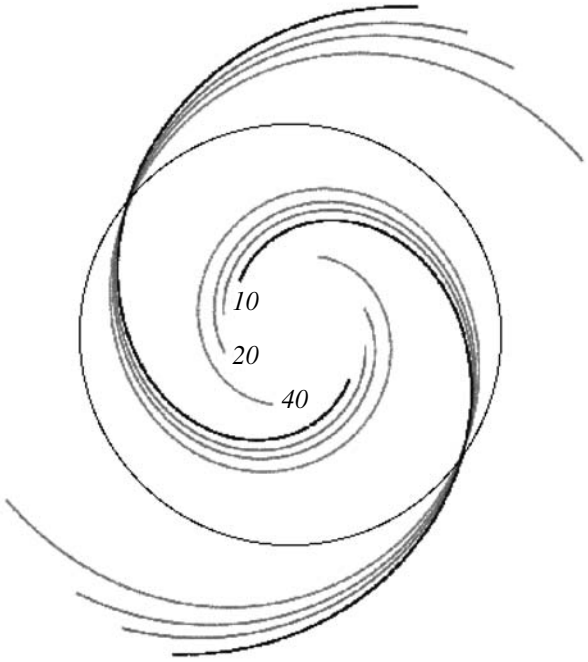


**Fig. 1.** Spiral structure in the distribution of HMXBs. Different curves corresponds to the locations of objects with ages of *10*, *20*, and *40* Myr calculated using Eq. (2). The location of the region of ongoing star formation (black curve) is also shown. The circumference indicates the location of the corotation radius.

To estimate the displacement of X-ray sources relative to the galactic spiral structure, we calculated the expected spatial distributions of HMXBs with ages of 10, 20, and 40 Myr. As the region of ongoing star formation, we used the approximation of the inner part of the star-forming region in M51 (see below) by a logarithmic spiral ($\psi = 19°$). The displacement of HMXBs relative to the instantaneous location of the spiral was calculated using Eq. (2) by assuming that the rotation curve and the density wave pattern speed also corresponded to those of M51. The derived distributions together with the current location of the spiral structure are shown in Fig. 1.

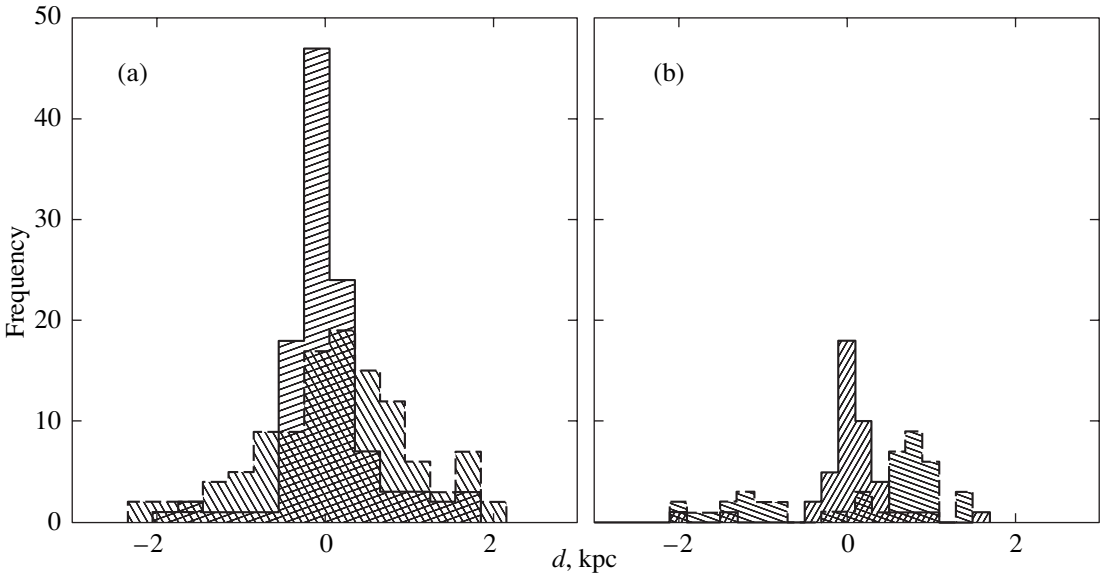


**Fig. 2.** (a) Distribution of distances from bright H II regions (Petit et al. 1996) to the nearest spiral arm (solid histogram) in M51. Also shown is the distribution for objects with an age of 40 Myr (dotted histogram). (b) The same for objects within the corotation radius.

## THE SPIRAL STRUCTURE AND HIGH-MASS X-RAY BINARIES: COMPARISON WITH OBSERVATIONS

Various methods can be used to study the spiral structure in the observed distribution of sources or emission intensity at a certain wavelength. For example, the distribution of displacements of the polar angle relative to the spiral angle, $\chi = \phi - \ln(r/r_0)/\tan\psi$, can be constructed. In this presentation method, a logarithmic spiral with two arms is projected into two $\delta$ functions near 0 and $\pi$. However, when the shape of the spiral structure is far from a logarithmic spiral, it is convenient to use the distributions of source distances to it. Obviously, this distribution will change in pattern as the sources "grow old". This effect can be demonstrated with an actual example using bright H II regions, for which the distribution of distances to the nearest spiral arm characterizes the locations of the youngest objects. The distribution for older objects can be obtained by displacing their locations relative to the current location of the spiral in accordance with Eq. (2). For this kind of demonstration, we chose bright H II regions in M51 ($S > 1.5 \times 10^{-17}$ W m$^{-2}$) from the catalog by Petit et al. (1996) and displaced them by assuming that the spiral was a trailing one (i.e., the rotation is counterclockwise; see Fig. 3). We then constructed the distributions of distances from the original and displaced sources to the nearest spiral arm (for more detail on the spiral structure in M51, see below) for sources in a wide range of galactocentric distances, 2.3 kpc $< r <$ 9.5 kpc, and within the corotation radius, 2.3 kpc $< r <$ 5.6 kpc. A distortion of the distribution is clearly seen in both cases (see Fig. 2); in the latter case, it is in the form of a displacement.

Obviously, for comparison with the qualitative model constructed above, a galaxy with active star formation and a low stellar mass whose spiral structure is close to a logarithmic spiral with a large pitch angle would be ideal. In addition, it is desirable that the angular size of the galaxy should be small enough for the contribution from background sources to be at a minimum.

### *Comparison with observations: M51*

One of the most suitable galaxies for our purpose among those observed by Chandra is M51. This galaxy has a distinct spiral structure and is located at a distance of 9.7 Mpc (Sandage and Tammann 1975). The displacements of various indicators of the spiral structure in M51 clearly indicate that we are dealing with a density wave (see, e.g., Tilanus and Allen 1989, 1991). To determine the orientation of M51 in space, we take the coordinates of its center $\alpha(\mathrm{J2000}) = 13^{\mathrm{h}}29^{\mathrm{m}}52\overset{\mathrm{s}}{.}71$ and $\delta(\mathrm{J2000}) = 47^\circ 11' 42\overset{''}{.}6$ (Ford et al. 1985) and its inclination to the plane of the sky $i = 20^\circ$ (Tully 1974). As the spiral wave pattern speed, we use $\Omega_\mathrm{p} = 38$ km s$^{-1}$ kpc$^{-1}$ obtained by Zimmer et al. (2004) by the Weinberg–Tremain method. Data on the rotation curve were taken from Tilanus and Allen (1991) and fitted by the law $V(r) \propto \sqrt{(r/r_0)^{1.3}/[1 + (r/r_0)^{2.3}]}$. The rotation curve and the density wave pattern speed correspond to a

corotation radius $r_{cr} \approx 5.6$ kpc, in agreement with the values obtained by other methods (Vogel et al. 1993).

An important peculiarity of M51 is its interaction with its companion, NGC 5195. As a result, it is often cited as an example of a galaxy where the spiral structure can be excited and maintained by tidal forces (see, e.g., Toomre 1978). The tidal interaction is probably also responsible for the unusually high density contrast in the $K$ band and, hence, in the stellar population of M51 (Rix and Rieke 1993). Obviously, a high density contrast in the stellar disk can change radically the manifestation of the spiral structure in X-ray binaries. For example, it would be natural to expect the appearance of a spiral structure in the distribution of not only HMXBs, but also LMXBs.

The spiral structure in M51 is more complex in shape than a simple logarithmic spiral and can be approximated by the latter only in a limited range of radii. Moreover, the ionized gas velocity field on the periphery of M51 indicates that the outermost parts of the spiral rotate with a pattern speed different from that of the inner spiral (Vogel et al. 1993).

Below, we exclude the region around NGC 5195 with a radius of $\approx 1'.7$ from our analysis.

**X-ray sources toward M51.** For our analysis, we used the list of sources detected by Chandra (Terashima and Wilson 2004). The total number of sources within a galactocentric radius of $\approx$10 kpc is 88 at the limiting sensitivity $S_{\rm lim} = 1.4 \times 10^{-15}$ erg cm$^{-2}$ s$^{-1}$ in the 0.5–8 keV energy band (for a photon index of 1.5 and $N_{\rm H} = 1.3 \times 10^{20}$ cm$^{-2}$), corresponding to the luminosity $L_{\rm X} = 1.6 \times 10^{37}$ erg s$^{-1}$. As with any other galaxy, most of the X-ray sources toward M51 belong to one of the following classes: HMXBs, LMXBs, SNRs, and background active galactic nuclei (AGNs). Below, we discuss the contribution from each of them to the population of X-ray sources toward M51.

(1) AGNs. According to the curve of background source number counts by Moretti et al. (2003), $N^{\rm s}_{\rm CXB} \approx 13$ cosmic X-ray background (CXB) sources are expected in a circle with a radius of $3'.4$ if we use the count curve in the soft 0.5–2 keV energy channel ($S^{\rm s}_{\rm lim} = 4.62 \times 10^{-16}$ erg cm$^{-2}$ s$^{-1}$, assuming $\alpha = 1.5$ and $N_{\rm H} = 1.3 \times 10^{20}$ cm$^{-2}$) and $N^{\rm H}_{\rm CXB} \approx 22$ background sources are expected if we use the count curve in the hard 2–10 keV energy channel ($S^{\rm H}_{\rm lim} = 1.17 \times 10^{-15}$ erg cm$^{-2}$ s$^{-1}$) with fluxes above the detection threshold.

A similar value, $N_{\rm CXB} \approx 18$, is obtained if we use the count curve in the 0.5–8 keV energy band obtained by Kim et al. (2006). We use this number below.

(2) HMXBs. To estimate the expected number of HMXBs, we use a calibration from Grimm et al. (2003) with a modified normalization (Shtykovskiy and Gilfanov 2005):

$$N(>L) = 1.8 \times SFR(L_{38}^{-0.6} - 210^{-0.6}), \qquad (3)$$

where $SFR$ is the star formation rate of the host galaxy.

According to the IRAS catalog (Rice et al. 1988), the far-infrared luminosity of M51 is $L_{\rm FIR} = 1.8 \times 10^{10} L_\odot$. The $L_{\rm FIR}$–$SFR$ calibration (Kennicutt 1998) yields $SFR \approx 3.1 M_\odot$ yr$^{-1}$. Using Eq. (3), we then obtain the expected number of HMXBs with luminosities above the detection threshold $S_{\rm lim}(2\text{–}10) = 1.17 \times 10^{-15}$ erg cm$^{-2}$ s$^{-1}$, $N_{\rm HMXB} \approx 19$. A slightly larger number is obtained if we use the star formation rate derived from the ultraviolet luminosity of M51, $SFR({\rm UV}) \approx 4.3 M_\odot$ yr$^{-1}$ (Calzetti et al. 2005), which corresponds to $N_{\rm HMXB} \approx 27$ HMXBs. However, this number is less reliable, because the absorption in the ultraviolet is uncertain.

It is worth noting that the calibration by Grimm et al. (2003) also includes the possible contribution from SNRs and ultrabright sources, which should be similar to HMXBs in spatial distribution.

(3) LMXBs. To estimate the number of LMXBs in M51, we use the fact that their number is proportional to the stellar mass of the galaxy (Gilfanov 2004). The latter, in turn, is proportional to the $K$-band flux (Bell and de Jong 2001). Using $K$-band images of M51 from the 2MASS Large Galaxy Atlas (Jarrett et al. 2003) and assuming that the magnitude in a $2'$ aperture is $K(<2') = 6.76$ (Rix and Rieke 1993), we obtain $K(r < 9.5\,{\rm kpc}) = 6.4$ for the entire galaxy. According to the calibration by Bell and de Jong (2001) and the color $(B-V)_0 = 0.56$ (de Vaucouleurs et al. 1991), this corresponds to $M_* = 2.63 \times 10^{10} M_\odot$. Using the galactic stellar mass–LMXB number calibration (Gilfanov 2004), we then obtain $N_{\rm LMXB} \approx 33$ (22 in the ring 2.3 kpc $< r <$ 9.5 kpc, 13 within the corotation radius 2.3 kpc $< r <$ 5.6 kpc) LMXBs with luminosities above the threshold value, $S_{\rm lim}(2\text{–}10) = 1.17 \times 10^{-15}$ erg cm$^{-2}$ s$^{-1}$.

Our estimates roughly agree with the observed total number of sources (see the table). The distribution of X-ray sources in M51 is shown in Fig. 3. It should be kept in mind that since the nucleus has a high X-ray brightness, Terashima and Wilson (2004) excluded the central part of the galaxy from their analysis. Therefore, the central depression in the number of sources should not be interpreted as the absence of X-ray binaries in this region.

**The spiral structure in the distribution of X-ray binaries.** It is natural to investigate the spiral

| Source class | HMXB | LMXB | CXB |
|---|---|---|---|
| Expected number of sources | 19–27 | 33 | 13–22 |
| Total observed number of sources | | 88 | |

structure in the distribution of X-ray binaries with respect to a certain indicator of the region of ongoing star formation or, in other words, an indicator of the shock front location. For example, the location of the most massive (and, accordingly, youngest) stars, the inner edge of the dust lane clearly seen in the $B$ band, the gas velocity distribution, etc. can serve as such an indicator. In our case, it is convenient to use the H$\alpha$ emission peak, which essentially reflects the location of the youngest stars, as the location of the spiral. For this purpose, we used the HST mosaic of M51 (Mutchler et al. 2005). The locations of the spiral arms drawn along the H$\alpha$ emission peak are indicated in Fig. 3 by the solid line. In addition, we used bright H II regions ($S > 1.5 \times 10^{-17}$ W m$^{-2}$) from the catalog by Petit et al. (1996) as an additional indicator.

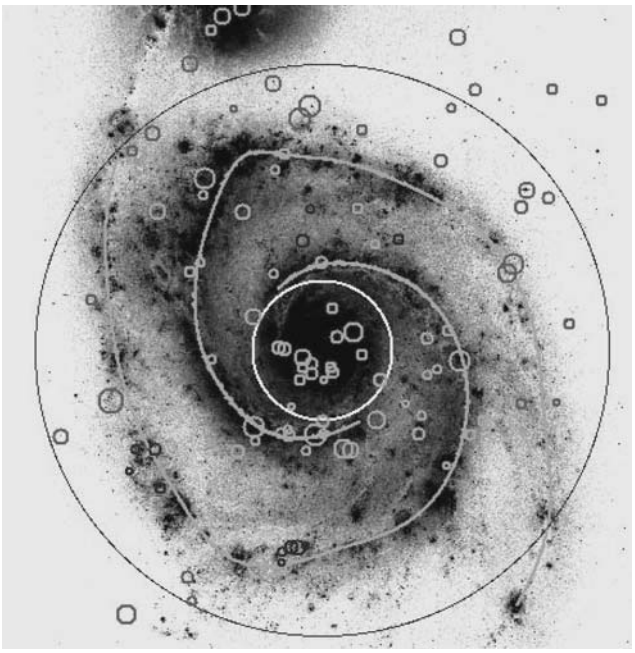

**Fig. 3.** HST H$\alpha$ image of M51 (Mutchler et al. 2005). The circles mark the positions of the X-ray sources detected by Chandra (Terashima and Wilson 2004); the circle radius reflects the source X-ray luminosity. For a higher contrast, the circles have different colors in different regions. Also shown are the two arms of the spiral structure used as the location of the region of ongoing star formation. The two circles around the galactic center (the light and dark ones at small and large distances, respectively) indicate the region from which the sources are taken for our analysis (2.3–9.5 kpc).

To estimate the degree of concentration of X-ray sources to the spiral arms, we calculated the distribution of their distances to the nearest spiral arm using sources at galactocentric distances 2.3–9.5 kpc. Positive and negative distances are assigned to sources above and below the spiral, respectively. The derived distribution (corrected for the galaxy inclination) is shown in Fig. 4.

Despite the obvious physical meaning of the constructed distribution, the interpretation of its shape is nontrivial. Indeed, a solid angle can be associated with each interval of distances on it. As a result, the solid angles for different intervals can differ; the distributions in this representation will be distorted, more specifically, they will be more concentrated to zero than they actually are. For example, a uniform distribution of sources, such as AGNs, will have a maximum near zero whose distinctness will be determined by the shape of the spiral and by the boundaries of the region from which the X-ray sources are taken. As a result, the observed distribution will have a clear meaning only when it is considered in comparison with another, "calibration", distribution. Obviously, in our case, the distribution of bright H II regions and a uniform distribution are such distributions.

The observed distribution is determined by the following factors.

(1) Finite width of the star-forming region. Even if the star formation in gas clouds is assumed to be triggered at a narrow shock front, the star formation process is not an instantaneous event, which smears the spatial region of zero-age stars. As was noted above, we consider our distribution relative to the distribution of H II regions, which, obviously, will reflect the width of the star-forming region. To make a quantitative comparison of the distribution for HMXBs with the distribution for H II regions possible, we normalized the latter to the difference between the total number of X-ray sources and the expected number of LMXBs and AGNs.

(2) Dynamics of HMXBs. The distortion of the distance distribution due to the displacement of sources relative to the region of ongoing star formation was demonstrated above. The expected distribution of HMXBs with allowance made for their dynamics is shown in Fig. 2. A characteristic feature of the distribution is its asymmetry, which is particularly noticeable if only the sources within the corotation radius are taken into account. In addition, the distribution of HMXBs is spread due to the initial velocities acquired through supernova explosions.

(3) LMXBs. As was noted above, a high stellar density contrast in M51 ($\delta\sigma/\sigma \sim 2$–3, mainly within

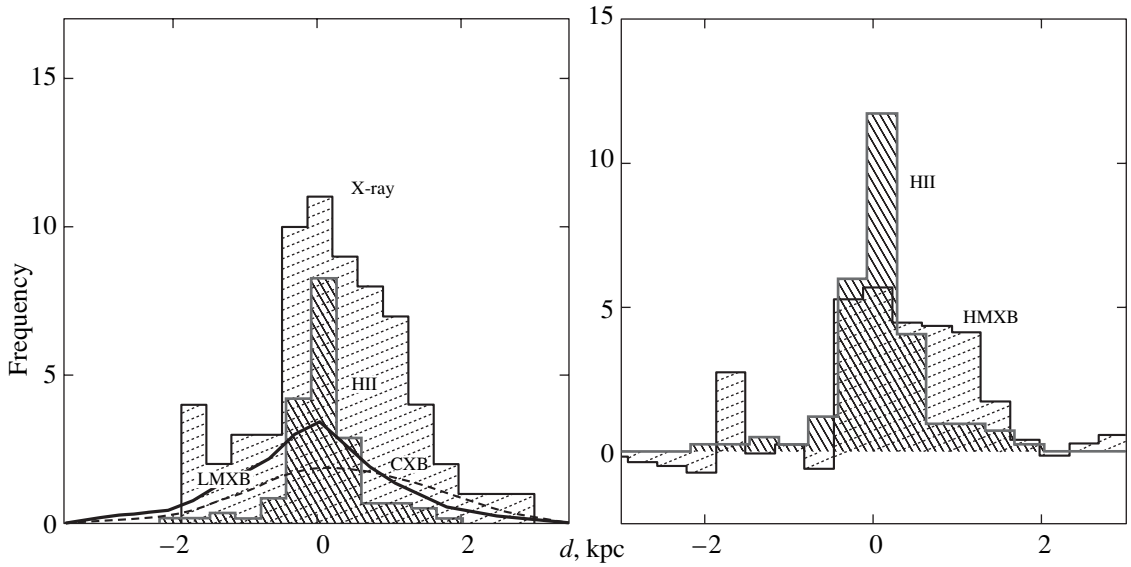


**Fig. 4.** (a) Distribution of distances to the nearest spiral arm for X-ray sources (wide histogram) and bright H II regions (narrow histogram, reverse hatching). The distribution for H II regions is normalized to the difference between the total number of X-ray sources and the expected number of LMXBs and AGNs. The solid and dotted curves correspond to the predictions for LMXBs and AGNs, respectively. (b) The difference between the distribution of X-ray sources and the total distribution of LMXBs and AGNs (wide histogram) and the distribution of bright H II regions (narrow histogram, reverse hatching).

the corotation radius) should lead to a concentration of these sources to the spiral arms. Obviously, their spatial distribution should differ from the observed one for HMXBs. To estimate the distribution of LMXB distances to the nearest spiral arm, we generated a model population of sources distributed over the galaxy in accordance with the K-band flux. The number of sources is taken to be large ($\approx 10^5$) to suppress the contribution from the Poisson noise. The derived distribution for the model sources was normalized in accordance with the expected number of LMXBs, $N_{\rm LMXB} = 22$.

(4) Contribution from background sources. To estimate the contribution from background sources, we calculate the distribution of distances to the nearest spiral arm for sources distributed uniformly over the sky and normalize it to the predictions of the count curves (see above), $N_{\rm CXB} = 18$.

The above components are shown in Fig. 4. Obviously, the distribution of X-ray sources is wider and more asymmetric than that of H II regions. This is the result of a cumulative effect from LMXBs, AGNs, and HMXB dynamics. To estimate the contribution from HMXBs, we give the difference between the distribution of X-ray sources and the sum of the predicted distributions for LMXBs and AGNs. The derived distribution is also asymmetric; it is similar in pattern to the prediction of the simplest model for the displacement of HMXBs (Fig. 2). However, the result is statistically insignificant. The significance of the fact that the distribution of X-ray sources is not a sample from the total distribution of LMXBs, AGNs, and bright H II regions calculated by Cooper's test is less than $2\sigma$ ($p \approx 13\%$).

Interestingly, the formal significance of the concentration of X-ray sources to the spiral arms is also low, although the reverse seems to be true at first glance at Fig. 3. Indeed, judging by Fig. 3, the density of sources near the spiral arms clearly exceeds their density in the interarm space. If we do a quantitative count, then we will find that almost as many sources are observed within a strip of $\pm 600$ pc as outside it,— 34 versus 32. At the same time, the corresponding areas are 11.1 versus 19.7 square arcminutes. Thus, the concentration is actually present, but its statistical significance is low. The significance of the fact that the distribution of distances of X-ray sources to the nearest spiral arm is not a sample from the distribution of sources distributed uniformly over the sky calculated by Cooper's test is also found to be low, about $2\sigma$ for sources with 2.3 kpc $< r <$ 9.5 kpc and slightly higher for sources within the corotation radius. Thus, the existing number of sources is clearly not enough to reach firm conclusions about the distribution of HMXBs relative to the spiral arms in M51. Moreover, as we said above, M51 is one of the best examples for studying the spiral structure among the galaxies observed by Chandra. Although a comprehensive analysis of the archival data on other spiral galaxies is beyond the scope of this paper, we expect

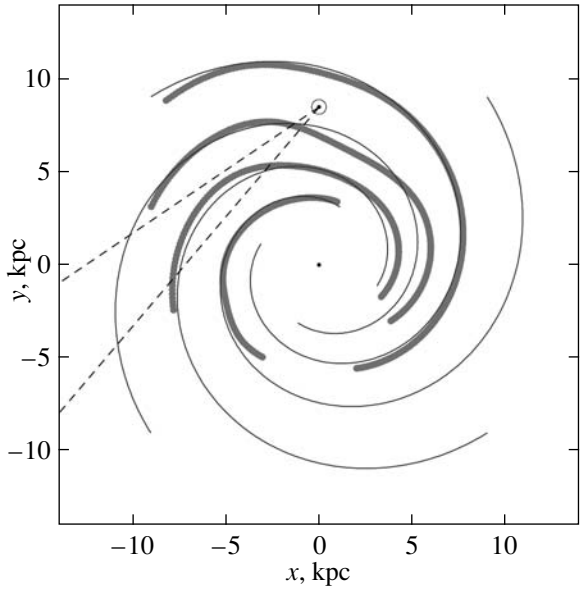


**Fig. 5.** Approximation of the spiral structure of our Galaxy by a logarithmic spiral and a model of th spiral structure from Taylor and Cordes (1993) (thick curve). The location of the Solar system and the solid angle containing the tangent to one of the spiral arms are shown.

the statistical significance of the manifestation of a spiral structure in X-ray sources in them to be even lower. Further deep Chandra observations of spiral galaxies with intense star formation are required to investigate the manifestation of the spiral structure in the distribution of X-ray sources in more detail.

### *High-Mass X-ray Binaries in our Galaxy*

The simplest kinematic model constructed here also allows us to make predictions about the expected distribution of HMXBs in our Galaxy observed from the Solar system ($r_\odot = 8.5$ kpc). For this purpose, we assume that the spiral structure of our Galaxy follows a logarithmic spiral with four arms and a pitch angle $\psi = 13^\circ$ that originates at a Galactocentric distance of 3.3 kpc (see, e.g., Vallee 2005, 1995) (Fig. 5). Figure 5 also presents a model of the spiral structure in the distribution of free electrons in the Galaxy from Taylor and Cordes (1993). Obviously, its shape deviates from a logarithmic spiral only slightly. We assume that the SFR and, accordingly, the number of HMXBs along the spiral arm length element decrease with decreasing exponential Galactic disk density. The characteristic width of the spiral arm is taken to be $w = 0.3$ kpc ($FWHM = 0.7$ kpc). The SFR at an arbitrary point in the Galaxy is calculated as follows:

$$SFR \propto \int e^{-r/r_0} \times e^{-d^2/2w^2} \times dl, \qquad (4)$$

where the integral is taken along the spiral arms, $dl$ is the length element of the spiral arm, $r$ is its Galactocentric distance, $d$ is the distance from the point to the spiral arm, and $r_0 = 3.9$ kpc (Benjamin et al. 2005).

After their birth, the HMXBs are displaced relative to the instantaneous locations of the spiral arms in accordance with Eq. (2). The rotation curve is assumed to be flat in the galactocentric distance range of interest, $V/(220\ \mathrm{km\ s^{-1}}) = a_1(R/8.5\ \mathrm{kpc})^{a_2} + a_3$ ($a_1 = 1.00767$, $a_2 = 0.0394$, $a_3 = 0.00712$) (Brand and Blitz 1993); as the spiral density wave pattern speed, we take $\Omega_\mathrm{p} = 24$ km s$^{-1}$ kpc$^{-1}$ (Dias and Lepine 2005), which corresponds to the corotation radius $\kappa_\mathrm{cr} \approx 9.3$ kpc.

Having integrated the SFR along the line of sights emanating from the Solar system, we obtained the distribution of HMXBs in Galactic longitude. The distributions for objects with ages of 0, 40, and 80 Myr constructed by assuming that we are capable of detecting only sources at heliocentric distances smaller than 6.5 and 11.5 kpc are shown in Fig. 6. The detection limits roughly correspond to the depths of the INTEGRAL survey for sources with luminosities $L_\mathrm{X} = 10^{35}$ and $10^{35.5}$ erg s$^{-1}$ (Lutovinov et al. 2005). As might be expected, the positions of the maxima in the distribution for the youngest objects correspond to the spiral arm tangents (see Fig. 5), since in this case the integrated SFR along the line of sight is at a maximum. At the same time, as we see from Fig. 5, the maxima in the distribution of older objects can be displaced significantly. Besides, additional peaks related to the fact that the hitherto invisible inner parts of the spiral arms become visible appear.

Obviously, the weakness of the constructed model is that we do not know the exact shape of the spiral arms and the SFR behavior along them. Indeed, if the SFR is highly nonuniform along the spiral arms, then the maxima in the distributions of young sources can also be observed in directions different from the spiral arm tangents.

The displacement of the HMXB maxima relative to the locations of the spiral arm tangents were actually observed by Lutovinov et al. (2005) (see Fig. 7 in this paper, the peak in a direction $l \approx +40^\circ$). The observed position of the peak corresponds to binaries with ages ≈40–80 Myr, which corresponds to the oldest binaries from the standpoint of HMXB evolution. However, to reach specific conclusions, we must primarily have a larger number of sources and, in addition, understand what contribution the SFR nonuniformity along the spiral arms makes to the distribution.

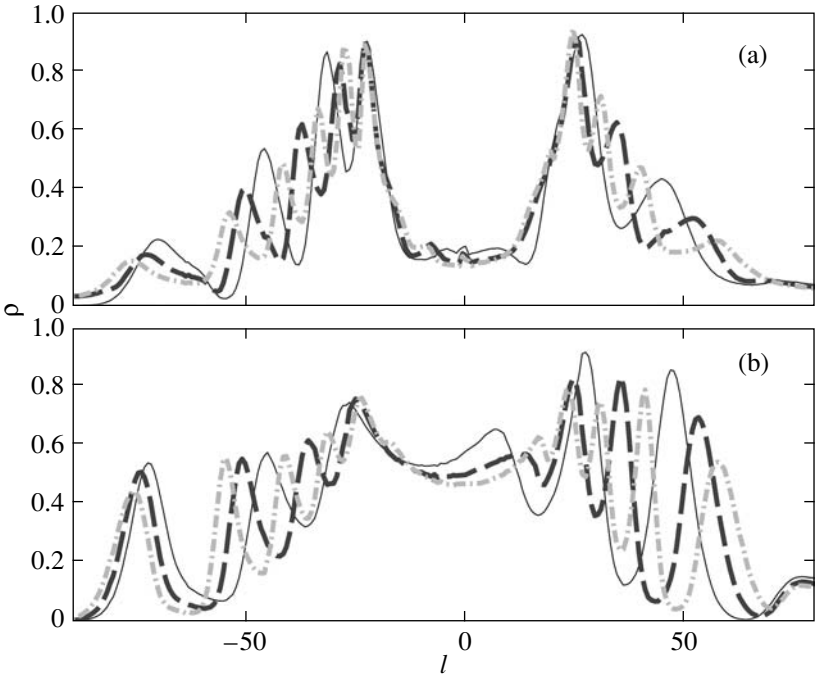


**Fig. 6.** Model distribution of HMXBs in our Galaxy in longitude for objects with ages of 0 (solid curve), 40 (dotted curve), and 80 Myr (dashed–dotted curve). Obviously, the solid curve describes the manifestation of the spiral structure in the youngest indicators, such as the $H_\alpha$ line and the distribution of the most massive early-type stars. We see that the peaks in the distribution of HMXBs are displaced considerably as the latter "grow old". The distributions were constructed for sources closer than (a) 11.5 and (b) 6.5 kpc.

## CONCLUSIONS

We considered the spatial distribution of HMXBs relative to the spiral structure of the host galaxy. We constructed the simplest model for the kinematics of HMXBs. It shows that they can be displaced to an appreciable distance from the location of the shock front at which ongoing star formation takes place over their lifetimes (see Figs. 1 and 2). As a result, the spiral structure in the distribution of HMXBs can be displaced relative to the spiral structure observed in classical SFR indicators, such as the H$\alpha$ emission. The displacement should be most pronounced for binaries with neutron stars and minimal for binaries with black holes. The evolution of the HMXB number with time elapsed since the star formation event can be judged by the displacement pattern.

As an illustration of this effect, we considered the spatial distribution of X-ray sources in the galaxy M51 by analyzing the distribution of their distances to the spiral arms. We showed that the components attributable to HMXBs and LMXBs and background AGNs could be identified in the distribution using $K$-band data and background source number counts. The distribution of HMXBs shows a clear tendency for them to concentrate to the spiral arms. In agreement with predictions of the kinematic model, it is wider and more asymmetric than the distribution of bright H II regions, which reflects the region of ongoing star formation (see Figs. 2 and 4). However, the statistical significance of both the concentration of X-ray sources to the spiral arms and the fact that the distribution of HMXBs differs from that of bright H II regions is low ($\lesssim 2\sigma$). Further deep Chandra observations of spiral galaxies are required to reach firm conclusions about the distribution of HMXBs relative to the spiral arms.

We also calculated the expected distribution of HMXBs in our Galaxy observed from the Solar system. We showed that the maximum number of sources could be observed in directions different from the directions tangential to the spiral arms, where the integrated current SFR is at a maximum (Fig. 6), because the HMXBs are displaced relative to the shock front. The displacement pattern allows the peculiarities of the HMXB distribution observed by Lutovinov et al. (2005) to be explained qualitatively.

## ACKNOWLEDGMENTS

P.E. Shtykovskiy thanks the European Association for Research in Astronomy (EARA; MESTCT-2004-504604) for support by a Marie Curie grant and the Max-Planck-Institut für Astrophysik, where this work was performed, for hospitality. This work was also supported by grant

no. NSh-1100.2006.2 from the President of Russia and the Russian Academy of Sciences ("Origin and Evolution of Stars and Galaxies" Program).

## REFERENCES


1. E. F. Bell and R. S. de Jong, Astrophys. J. **550**, 212 (2001).
2. R. A. Benjamin, E. Churchwell, B. E. Babler, et al., Astrophys. J. Lett. **630**, 149 (2005).
3. J. Brand and L. Blitz, Astron. Asrophys. **275**, 67 (1993).
4. D. Calzetti, R. C. Jr. Kennicutt, L. Bianchi, et al., Astrophys. J. **633**, 871 (2005).
5. W. S. Dias and J. R. D. Lepine, Astrophys. J. **629**, 825 (2005).
6. G. Fabbiano, Ann. Rev. Astron. Astrophys. **44**, 323 (2006).
7. H. C. Ford, P. C. Crane, G. H. Jacoby, et al., Astrophys. J. **293**, 132 (1985).
8. M. Gilfanov, Mon. Not. R. Astron. Soc. **349**, 146 (2004).
9. H. J. Grimm, M. Gilfanov, and R. Sunyaev, Mon. Not. R. Astron. Soc. **339**, 793 (2003).
10. T. H. Jarrett, T. Chester, R. Cutri, et al., Astron. J. **125**, 525 (2003).
11. R. C. Kennicutt, Jr., Ann. Rev. Astron. Astrophys. **36**, 189 (1998).
12. R. E. Kilgard, J. J. Cowan, M. R. Garcia, et al., Astrophys. J., Suppl. Ser. **159**, 214 (2005).
13. M. Kim, B.J. Wilkes, D.-W. Kim, et al., Astrophys. J. (in press); astro-ph/0611841.
14. D. Leisawitz and F. Bash, Astrophys. J. **259**, 133 (1982).
15. C. C. Lin and F. H. Shu, Astrophys. J. **140**, 646 (1964).
16. C. C. Lin and F. H. Shu, Proc. Natl. Acad. Sci. USA **55**, 229 (1966).
17. C. C. Lin, C. Yuan, and F. H. Shu, Astrophys. J. **155**, 721 (1969).
18. A. Lutovinov, M. Revnivtsev, M. Gilfanov, et al., Astron. Astrophys. **444**, 821 (2005).
19. A. Moretti, S. Campana, D. Lazzati, et al., Astrophys. J. **588**, 696 (2003).
20. M. Mutchler, S. V. W. Beckwith, H. Bond, et al., Bull. Am. Astron. Soc. **37**, 452 (2005).
21. H. Petit, C. T. Hua, D. Bersier, et al., Astron. Astrophys. **309**, 446 (1996).
22. K. A. Postnov, Astron. Lett. **29**, 372 (2003).
23. W. Rice, C. J. Lonsdale, B. T. Soifer, et al., Astrophys. J., Suppl. Ser. **68**, 91 (1988).
24. H.-W. Rix and M. J. Rieke, Astrophys. J. **418**, 123 (1993).
25. W. W. Roberts, Astrophys. J. **158**, 123 (1969).
26. W. W. Roberts, Jr., and G. R. Stewart, Astrophys. J. **314**, 10 (1987).
27. A. Sandage and G. A. Tammann, Astrophys. J. **196**, 313 (1975).
28. P. Shtykovskiy and M. Gilfanov, Astron. Astrophys. **431**, 597 (2005).
29. P. Shtykovskiy and M. Gilfanov, Pis'ma Astron. Zh. (2007) (in press).
30. J. H. Taylor and J. M. Cordes, Asrophys. J. **411**, 674 (1993).
31. Y. Terashima and A. S. Wilson, Astrophys. J. **601**, 735 (2004).
32. R. P. J. Tilanus and R. J. Allen, Astrophys. J. **339**, 57 (1989).
33. R. P. J. Tilanus and R. J. Allen, Astron. Astrophys. **244**, 8 (1991).
34. A. Toomre, in *Proceedings of the IAU Symposium No. 79,* Ed. by M. S. Longair and J. Einasto (Reidel, Dordrecht, 1978), p. 109.
35. R. B. Tully, Astrophys. J., Suppl. Ser. **27**, 437 (1974).
36. G. de Vaucouleurs, A. de Vaucouleurs, Jr. Corwin, et al., *Third Refererence Catalog of Bright Galaxies* (Springer-Verlag, New York, 1991).
37. J. P. Vallee, Astrophys. J. **454**, 119 (1995).
38. J. P. Vallee, Astron. J. **130**, 569 (2005).
39. S. N. Vogel, R. J. Rand, R. A. Gruendl, et al., Publ. Astron. Soc. Pac. **105**, 666 (1993).
40. P. Zimmer, R. J. Rand, and J. T. McGraw, Astrophys. J. **607**, 285 (2004).


*Translated by V. Astakhov*